

Precipitation Behavior of Ni-Fe Base Wrought Superalloy 706

Takashi Shibata*, Yukoh Shudo*, Tatsuya Takahashi*, Mikio Kusuhashi**,
Yuichi Yoshino***, Dr. Tohru Ishiguro****

—Synopsis—

Ni-Fe-base wrought superalloy 706 has been used for high temperature services. However, the precipitation behavior in this alloy system has not been well understood. Therefore, intensive TEM study was conducted in the present study to clarify the precipitation behavior of Alloy 706. Samples taken from a large gas turbine disk forging were treated either by two-step heat-treatment (solution and aging) or by three-step heat-treatment (solution, stabilizing and aging). In the former case, fine γ' - γ'' co-precipitates having the core of γ' being overlaid with γ'' on its top and/or bottom were identified in the matrix, and no precipitates were observed at the grain boundary. In the latter case, large cuboidal γ' - γ'' co-precipitates having the core of γ' being completely covered with γ'' were identified in the matrix together with fine overlaid co-precipitates, and η phase was identified at the serrated grain boundary accompanied by the denuded zone. Furthermore, in this study, the up-dated time-temperature-precipitation (TTP) diagrams of Alloy 706 were obtained in a temperature range from 600 to 900°C for up to 100h. In case of "On Heating TTP" diagram four types of precipitates appear, but in case of "On Cooling TTP" diagram five types of precipitates are present. The difference in the precipitation behavior between the two-step heat-treatment and the three-step heat-treatment can be explained by this TTP behavior.

1. Introduction

The tendency towards power generating plant with a high efficiency becomes more and more apparent for the reason of energy problem backed by the global environmental issues. The ultra- super critical pressure or the gas turbine power generating plant tends to require a higher operating temperature. As a consequence, the research and development of the materials for structural components such as the turbine rotors, turbine disks, blades is recognized as an important problem.

Fe base superalloy A 286 and Ni base superalloy Alloy 718 known representative wrought superalloy possess stable structure and high strength even at the extremely low temperature and high temperature environment. These superalloys are age-hardened by the precipitation of coherent γ' phase ($L1_2$, FCC like) and/or γ'' phase ($D0_{22}$, BCT like) in the austenitic matrix γ ¹⁾. Alloy 706 is a relatively new material and was developed from Alloy 718. Compared with Alloy 718, it has a chemical composition of no molybdenum, reduced nickel, chromium, niobium and carbon, and increased titanium and iron. This excellent balance of chemical composition results in superior characteristics to Alloy 718 in the segregation tendency, hot workability and machinability²⁻⁴⁾. Therefore, Alloy 706 is suitable for large forgings and

has been used for high temperature services^{5,6)}.

Alloy 706 is also precipitate strengthened alloy. However, the precipitation behavior in this alloy system has not been well understood. For example, it is reported that the intra-granular precipitate is either γ' ^(2,3,7,8) or γ'' ^(4,9,10) and simultaneously¹¹⁻¹⁶⁾. Likewise, the grain boundary precipitated phase are reported to be of η phase ($D0_{24}$, HCP like) or of δ phase ($D0_8$, orthorhombic), and which is correct is not clarified^{2-4,7-16)}. In addition to these unclearnesses, the intermediate heat treatment called a stabilizing treatment between solution-annealing and age-hardening treatment (this is called the three-step heat-treatment) might be given in Alloy 706, though a usual precipitate strengthened type alloy is manufactured from giving two kind of heat treatment, solution-annealing and age-hardening treatment (this is called the two-step heat-treatment). Naturally, the precipitation behavior of the Alloy 706 is presumed to change to a great extent but little attention has been given to the point.

On the other hand, it is necessary to know the TTP (time-temperature-precipitation) diagram to estimate the change of mechanical properties, namely the change of precipitation behavior. Although, several TTP diagrams of Alloy 706 have already

*Muroran Research Laboratory **R & D Headquarters ***New Business Promotion Office ****Forgings & Castings Division

been presented up to now^{2,3,15}), it is pointed out that correspondence with the precipitation behavior is not clear.

As already mentioned above, unclearness of precipitation behavior poses a big problem not only in the basic understanding of strengthening mechanism of Alloy 706 but also from practical viewpoint such as making of manufacturing method or development of new alloys, etc. Therefore, the authors have investigated the change in the precipitation behavior according to the heat treatment of Alloy 706 by using a high resolution type transmission electron microscope^{18–22}). The precipitation behavior of Alloy 706 is summarized in this report based on those results.

2. Procedure

The chemical composition of Alloy 706 used in this study is given in **Table 1**. The experimental material was taken from a large gas turbine disk manufactured from a vacuum induction melted (VIM) and electro slag remelted (ESR) ingot that was diffusion treated and subsequently forged. The material was sectioned mechanically into samples of suitable sizes for the following experiments.

As the two-step heat treatment, the solution treatment was conducted at 980°C for 3h and it was air cooled. Subsequently the sample was double-aged at 720°C for 8h and at 620°C for 8h and it was furnace cooled. As the three-step heat treatment, the sample was solution treated at 980°C for 3h and then stabilizing treated at 810°C for 1.5h and it was air cooled. Subsequently the sample was double-aged at 720°C for 8h and at 620°C for 8h and it was furnace cooled. Alloy 706 is usually reheated to the stabilizing temperature after solution annealing¹⁷). In this study, the stabilizing treatment was conducted in the cooling stage from the solution treatment without cooling the material to the room temperature from the point view of industrial advantage or prevention of the strain induced precipitation²³).

In order to clarify the TTP Behavior, heat treatment was performed under two conditions. In one condition, after solution heat treatment at 980°C for 3h, samples were isothermally heat treated in a temperature range of 600–900°C for up to 100h (herein-

after referred to On Heating TTP). In the other condition, after the solution treatment at 980°C for 3h, the samples were cooled down to various temperatures between 900 and 600°C and held isothermally up to 100h (hereinafter referred to On Cooling TTP).

The heat treated samples etched with 50% aqua regina ethanol solution after the polishing of the mirror side, and observed the precipitation behavior by scanning electron microscope (SEM). In addition, the thin samples made by electro-polishing with 10% sulfuric acid ethanol solution or 5% perchloric acid acetic acid solution were observed by a transmission electron microscope (TEM). A 200kV TEM was used with micro-beam technique in both electron diffraction and energy dispersive X-ray spectroscopy (EDS), with the probe diameter being 0.5–5nm.

3. Result and Discussion

3.1 Precipitates that appear in Alloy 706 treated with the two-step heat treatment

SEM micrograph of the two-step heat treated Alloy 706 is shown in **Fig 1**. No precipitate was seen inside the grains or at the grain boundary in SEM order. In addition, the precipitate was not observed in the grain boundary as for the observation by TEM order. It is reported that the grain boundary precipitation of carbides is identified sometimes in Alloy

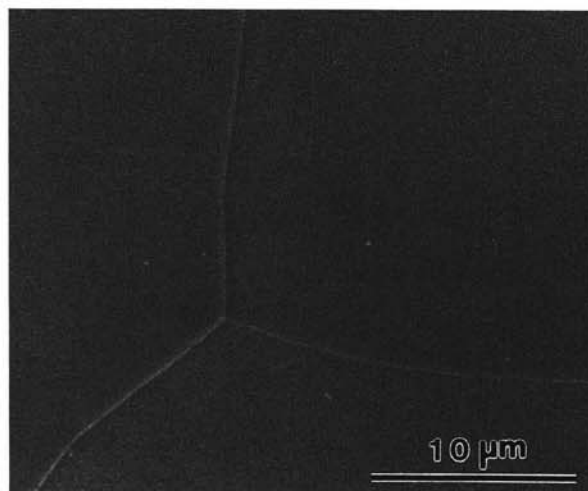


Fig. 1 SEM micrograph of Alloy 706 treated with the two-step heat treatment

Table 1 Chemical composition of test material

(mass %)												
Ni	Fe	Cr	Al	Ti	Nb	B	C	N	Si	Mn	P	S
42.00	37.10	15.65	0.26	1.54	2.96	0.0034	0.008	0.0046	0.05	0.02	0.003	0.0005

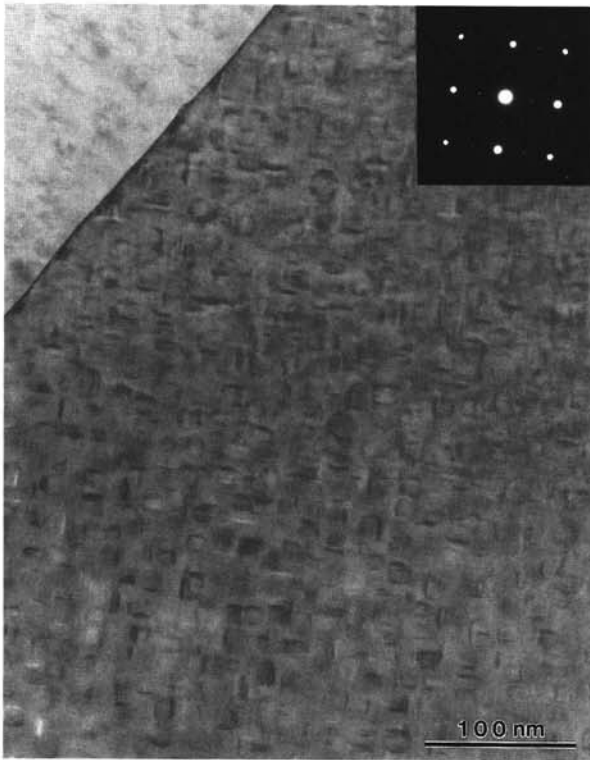


Fig. 2 TEM micrograph of Alloy 706 treated with the two-step heat treatment

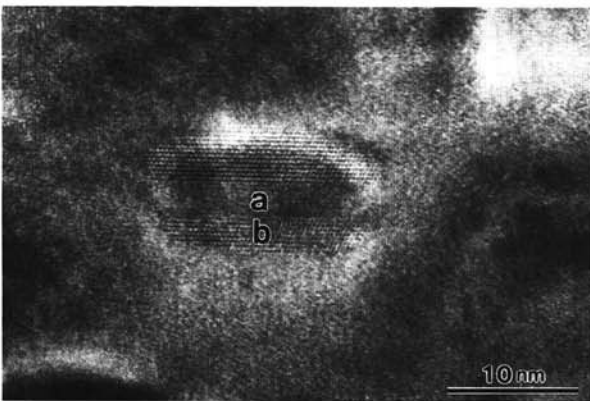


Fig. 3 High resolution TEM image of the precipitates that appear in the matrix of Alloy 706 treated with the two-step heat treatment

706^{7,9,15,16}). But scarcely any precipitation was observed in this study. It is considered that it is due to relatively low content of carbon in the Alloy 706 used in this study.

On the other hand, very fine precipitates of several nanometers was observed in the matrix as shown in Fig. 2. Fig. 3 shows a high-resolution image of this precipitates. From the continuity of crystal lattice, it is estimated that the structure of the core was different from that of its periphery. So we have

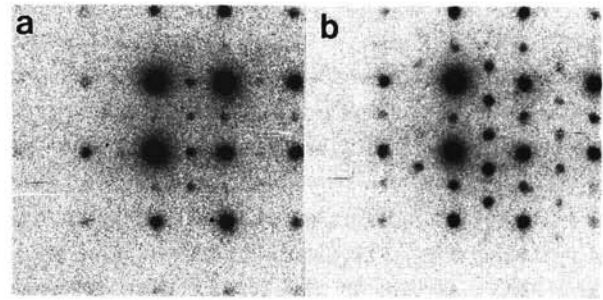


Fig. 4 Micro beam diffraction patterns at the locations shown in Fig. 3

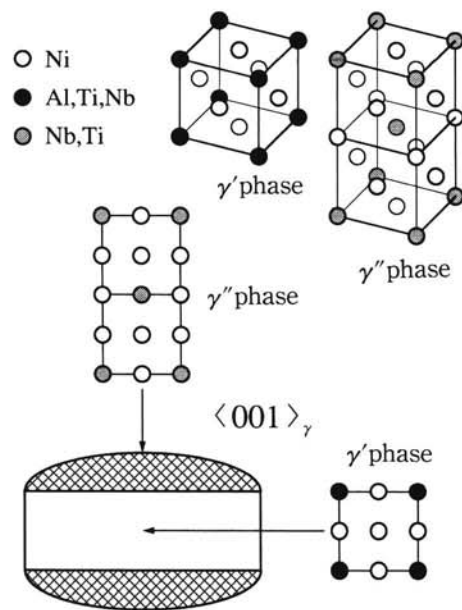


Fig. 5 Schematic diagram of the overlaid γ' - γ'' co-precipitation

conducted micro-beam electron diffraction on the core and the periphery. As it is shown in Fig. 4, it was possible to identify regular lattice reflection corresponding to γ' in the core and to γ'' in the periphery and it was made clear that the coherency between γ , γ' and γ'' was maintained. Also, in some cases, this γ'' was identified only on one side of γ' . Though it was not possible to clarify its detailed shape and inner structure because this γ' - γ'' co-precipitate was very fine, it had the core of γ' being overlaid with γ'' on its both side or either side keeping a specific orientation relationship as shown in Fig. 5. Although most of the precipitates in the matrix were identified to be this overlaid γ' - γ'' co-precipitates, a part of them were identified to be γ'' Precipitates.

From the results mentioned above, it was made clear that the precipitates in the matrix of Alloy 706

treated with the two-step heat treatment consisted predominantly of fine overlaid γ' - γ'' co-precipitates with a little co-existence of γ'' , and no precipitates were observed at the grain boundary. From the result of the observation before and after the aging treatment, it was made clear the fine precipitates in the matrix appeared at the stage of aging treatment^{18,22}.

3.2 Precipitates that appear in Alloy 706

treated with the three-step heat treatment

SEM micrograph of the three-step heat treated Alloy 706 is shown in **Fig. 6**. The precipitates were observed clearly in the grain matrix and at the grain boundary in case of the three-step heat treatment. Particularly, these precipitates appeared to originate at grain boundary in parallel to each other, which results in the wavy shape of grain boundary.

First, the identification result of the precipitate which appears at the grain boundary is described. **Fig. 7** shows the TEM observation result of the vicinity of the grain boundary of the three-step heat treated Alloy 706. The results of micro-beam electron diffraction revealed that these precipitates had Ni_3Ti type structure (η Phase: D_{024} , HCP like). The peak of Ni, Ti, and Nb was admitted from the compositional analysis result by EDS and the ratio between Ni and Ti + Nb was nearly 3:1. Therefore, it is thought that Nb is substituted for the Ti site. From the micro-beam selected area diffraction image in the vicinity of grain boundary shown in **Fig. 7**, the η phase had a specific orientation relationship with the γ matrix, as $[011]_{\gamma} // [2\bar{1}\bar{1}0]_{\eta}$ and $(11\bar{1})_{\gamma} // (0001)_{\eta}$. This relationship is consistent with the study concerning A286 and Alloy 706 reported by other^{1,9,14}, indicating a semi-coherency between η and γ .

It is reported that there is not only η , but also δ at the grain boundary at Alloy 706^{2-4,7,9,15,16}. However, no precipitate was identified δ for more than a hundred precipitates at grain boundary in this study. Some reports at the initial stage^{2,7,9} point out the limitation of TEM technology to distinguish η phase and δ phase. So it can be concluded that the η phase of the grain boundary precipitate in Alloy 706 is superior from the present study. Also, only a few precipitates were identified γ' in the sample. Therefore, this is thought that η forms through the transformation of $\gamma \rightarrow \gamma' \rightarrow \eta$ as in A286¹. The grain boundary appears to become serrated as the η phase grows as shown in **Fig. 7**. It is considered that this is due to the displacement of the grain boundary which is incidental to the growth of such η phase.

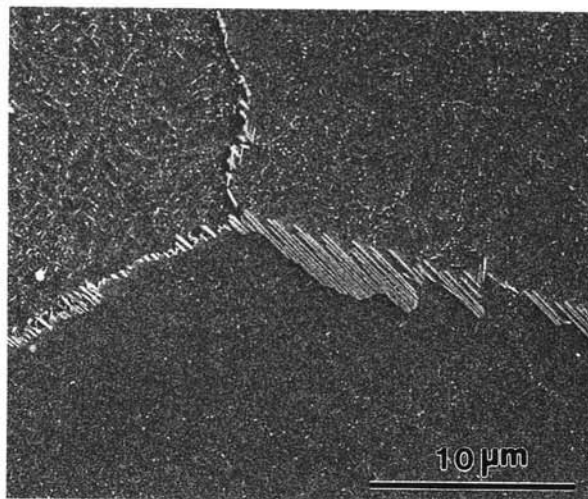


Fig. 6 SEM micrograph of Alloy 706 treated with the three-step heat treatment

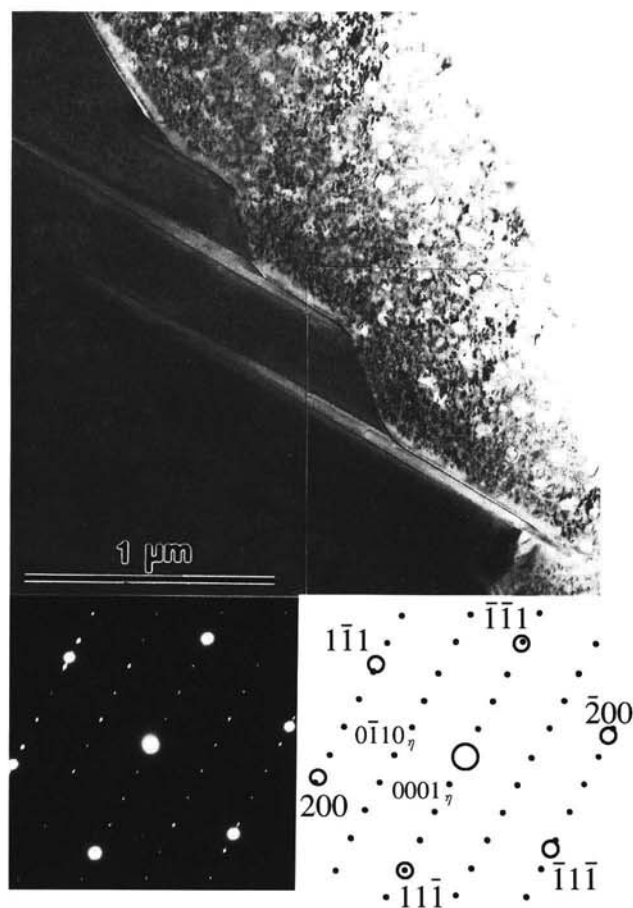


Fig. 7 TEM micrograph in the vicinity of grain boundary of Alloy 706 treated with the three-step heat treatment

As shown **Fig. 7**, the precipitation of η resulted in the formation of the serrated grain boundary and denuded-zone around it. It is reported that the identical denuded zone is caused along with the precipitation of the δ in Alloy 718²⁴) and it is considered that it is formed due to the reduction of Ti and Nb in the matrix with the growth of η .

Next, the identification result of intra-granular precipitates were described. TEM micrograph of the three-step heat treated Alloy 706 is shown in **Fig. 8**. The precipitates of various shapes and size exist inside the grain. The spots arising from long-range ordering were clearly observed in a selected area diffraction pattern, indicating the presence of γ' and/or γ'' . Therefore, high resolution observation was made together with micro-beam techniques in order to identify each precipitate. As a result, four types of precipitates were identified in the grain interior.

First of all, the precipitates as indicated by arrows a and b in **Fig. 8** were identified overlaid γ' - γ'' co-precipitates and γ'' that appeared in the case of the two-step heat treatment. Their sizes were several nanometers and they were very fine. The relatively large precipitates as indicated by arrow c were identified γ' , there size being several hundred nanometers. However, the number of large γ' were very few compared with the fine precipitates.

With respect to the relatively large precipitates in **Fig. 8**, the precipitates as indicated by arrow d was overwhelmingly preponderant in comparison to the one as indicated by arrow c. A high resolution image of this precipitate is shown in **Fig. 9**. It is guessed that this precipitates also has the combined structure

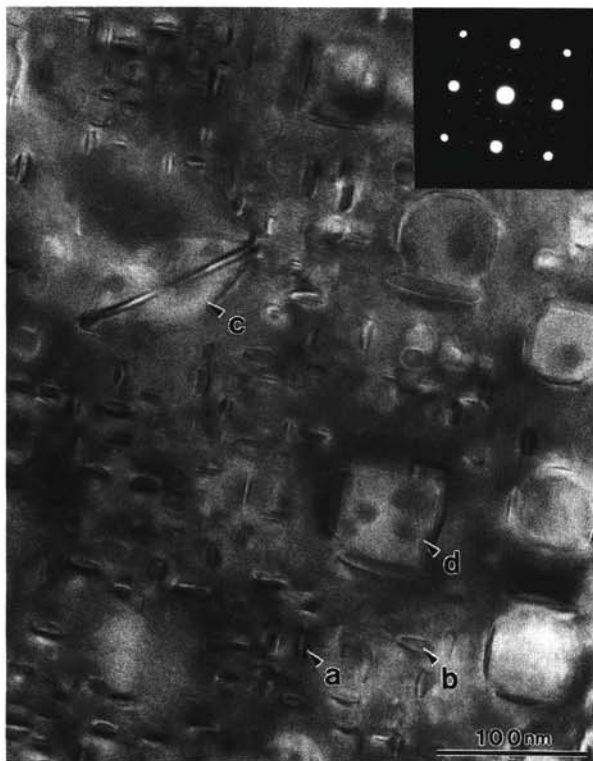


Fig. 8 TEM micrograph in the matrix of Alloy 706 treated with the three-step heat treatment

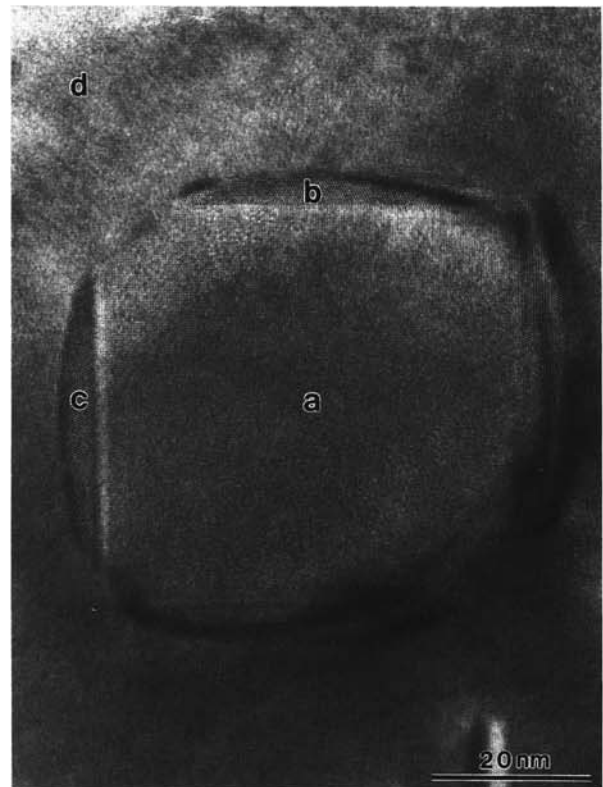


Fig. 9 High resolution image of the co-precipitate in the matrix of Alloy 706 treated with the three-step heat treatment (d in **Fig. 8**)

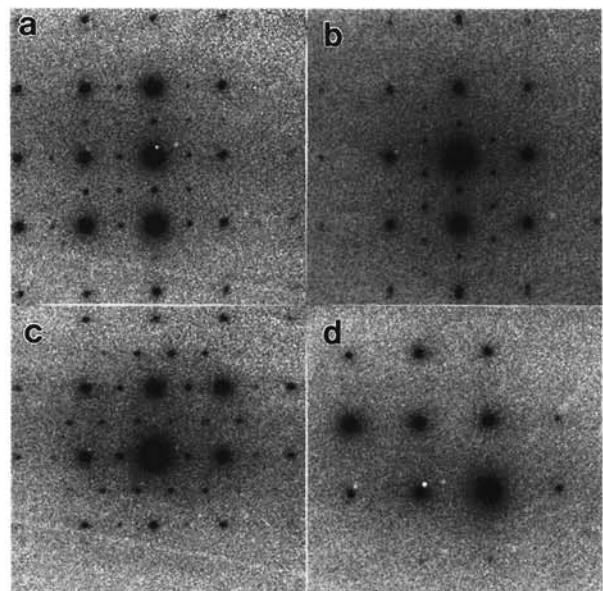


Fig. 10 Micro beam diffraction patterns at the location shown in **Fig. 9**

from the continuity of crystal lattice. Micro-beam electron diffraction patterns of each portion in **Fig. 9** are shown in **Fig. 10**. It was possible to identify regular lattice reflection corresponding to γ' in the core (a) and to γ'' in the periphery (b and c) and it

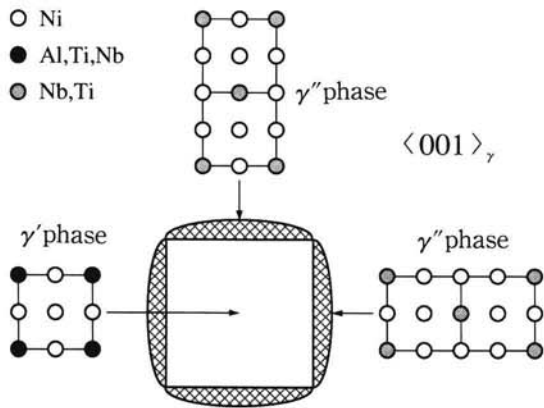


Fig. 11 Schematic diagram of the double cuboidal γ' - γ'' co-precipitate

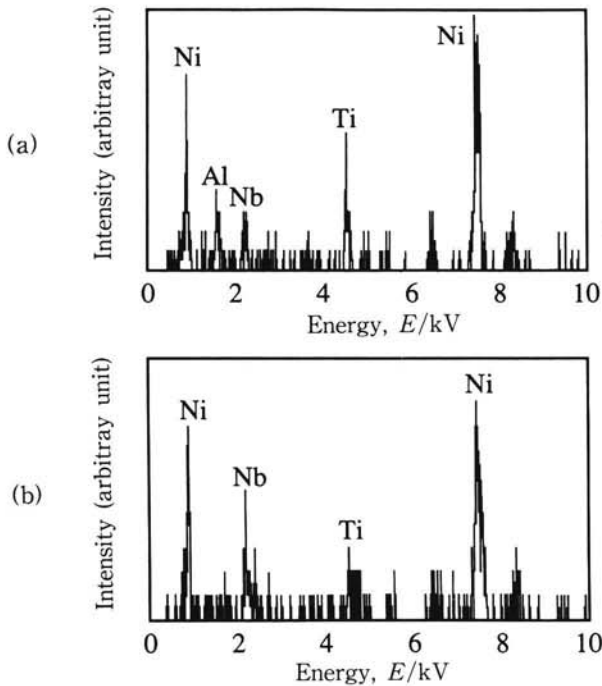


Fig. 12 Micro beam EDS spectra at the locations shown in Fig. 9

was made clear that the coherency between γ , γ' and γ'' was maintained as it was shown on the schematic diagram in Fig. 11. On the other hand, from the fact that the observation of co-precipitate as indicated by arrow d from multiple directions also revealed the existence of γ'' in the periphery. So, it is presumed that thin γ'' exist practically on the top and the bottom of γ' in the core. However, when they are in a orientation relationship as previously mentioned, γ'' and γ' overlaid along the axis c take nearly the same crystal structure, therefore, it is

presumed that we can observe only the regular lattice reflection corresponding to γ' in the center portion. Micro-beam EDS spectra of each section of this co-precipitation is shown in Fig. 12. The peaks of Ni, Ti, Nb and Al in the core and those of Ni, Ti and Nb in the periphery was observed. In either of the cases, the ratio between Ni and Ti+Nb (+Al) was 3:1. The comparison of Ti with Nb revealed that Ti was rich in the core while Nb was rich in the periphery. Therefore, in Alloy 706, it is presumed that a lot of Ti and Nb (particularly Ti) has substituted at Al site of γ' , while Ti has substituted at Nb site of γ'' .

From the result mentioned above, this precipitate was identified with the double cuboidal γ' - γ'' co-precipitates having the core of γ' being completely covered with γ'' thin skin.

Moreover, from the result of observation before and after the aging treatment, it was found out that the relatively large precipitates such as c and d, the precipitation of η and the change in grain boundary structure according to it had already appeared before the aging treatment, while the fine precipitates such as a and b had appeared at the stage of aging treatment like in the case of the two-step heat treatment^{18,22}). Therefore, it is suggested that, although overlaid precipitate and double cuboidal γ' - γ'' co-precipitate have nearly the same compound structure, their precipitations correspond to different heat treatments, namely, the difference of precipitation mechanisms. The precipitation behavior of the three-step heat treated Alloy 706 are strongly influenced by intermediate heat treatment which is stabilizing treatment. As a result, mechanical property like tensile properties and creep property, etc. change greatly, too. The details are recorded in another report due to the limited number of pages for this report^{10,19,12}).

3.3 TTP behavior of Alloy 706

As mentioned above, it was made clear that in the case of the two-step heat treatment, the precipitate in the matrix consisted predominately of overlaid γ' - γ'' co-precipitates, and no precipitates were observed at the grain boundary. On the other hand, it was made clear that in the case of the three-step heat treatment, precipitation in the matrix revealed the appearance of double cuboidal γ' - γ'' co-precipitate in addition to the overlaid γ' - γ'' co-precipitate, and η phase was identified at the serrated grain boundary accompanied by the denuded zone. In this section, the difference in the precipitation behavior between the two-step heat treatment and the three-step heat

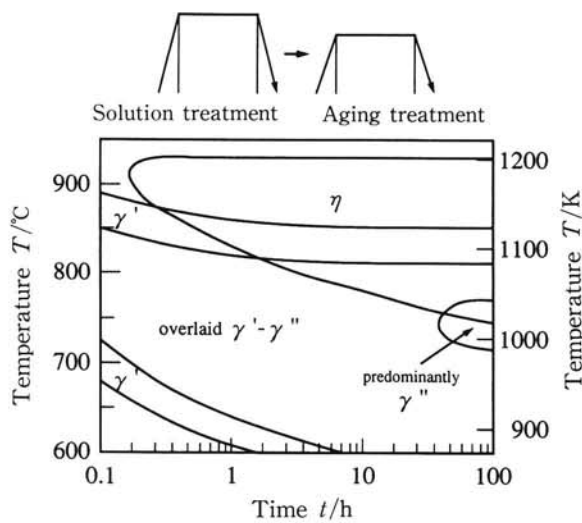


Fig. 13 "On Heating TTP" diagram of Alloy 706

treatment is discussed in accordance with the TTP behavior of Alloy 706.

"On Heating TTP" diagram is shown on Fig. 13. In several TTP diagrams of reported Alloy 706, it is reported that η , γ' , γ'' and carbide appeared as precipitates^{2,3,15}. However, in case of "On Heating TTP" diagrams, four type of precipitates appeared namely, η , γ' , γ'' and overlaid γ' - γ'' co-precipitate. It is considered that the intra-granular precipitate which appears by the aging treatment for 8h at 720°C and for 8h at 620°C used by this study is an overlaid γ' - γ'' co-precipitate from Fig. 13. As observed in this study, this is consistent with the prior appearance of the fine overlaid γ' - γ'' co-precipitates at the aging treatment of the two-step and the three-step heat treatment. The region of η precipitation grows wider as aging time increases. In fact, the η was found to shoot out from the grain boundary as the aging time increased at about 800°C. Therefore, the γ' , γ'' and overlaid γ' - γ'' co-precipitates all transform eventually to η when aged for long time at high temperature. The range of appearance of η phase precipitates is above 800°C for about several hours, and this corresponds to setting up the temperature of intermediate heat treatment (stabilizing treatment) usually at 840°C in the case of the three-step heat treatment¹⁷. It is corresponding to this research result in which the precipitation of η phase and the change of grain boundary appearing only at the three step heat treatment, and not appearing at the two step heat treatment.

However, the double cuboidal γ' - γ'' co-precipitate which appeared at the three-step heat treatment is

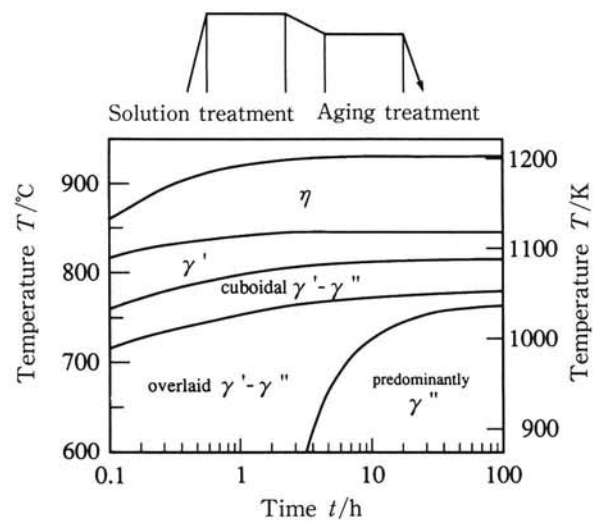


Fig. 14 "On Cooling TTP" diagram of Alloy 706

not admitted on "On Heating TTP" diagram in Fig. 13. It is suggested that this originates in continuous heat treatment of stabilizing treatment and solution treatment used in this study.

Now, "On Cooling TTP" diagram of Alloy 706 is shown in Fig. 14. While four types of precipitates appeared with "On Heating TTP" diagram, it was made clear that five types of precipitates appeared with "On Cooling TTP" diagram. Namely, in addition to η , γ' , γ'' and overlaid γ' - γ'' co-precipitates, double cuboidal γ' - γ'' co-precipitates appeared. This shows that the double cuboidal γ' - γ'' co-precipitates are occurred in the heat treatment process which is different from that of overlaid γ' - γ'' co-precipitates and that the growth mechanism is different. So, the growth mechanism of two co-precipitates will be discussed in the next paragraph.

3.4 Growth mechanism of co-precipitates

The appearance of the co-precipitate in the Ni base superalloy is reported in the process of the composition improvement in the modified 718 alloys²⁵⁻³². The overlaid γ' - γ'' co-precipitates and the double cuboidal γ' - γ'' co-precipitates admitted by this research are thought to be the same time as so called "non-compact morphology" and to "compact morphology" reported for the modified Alloy 718. According to those reports, it is reported that this co-precipitates is obtained at a higher (Al + Ti) / Nb ratio than in conventional Alloy 718. It is considered that this is attributable to the fact that, while Al and Ti are the forming element of γ' , Nb is the forming element of γ'' . In fact, with Nb free, only

γ' precipitates appear. On the contrary, with Al free, only γ' precipitates appear^{20,21}. It is necessary to improve the composition that the (Al+Ti)/Nb ratio becomes higher to facilitate the formation of the γ' because the γ'' precipitates are predominant in Alloy 718. In fact as a result of improving composition of Alloy 706 from viewpoint of segregation property and workability, (Al+Ti)/Nb ratio has become high in comparison to that of Alloy 718, it is sufficiently possible to predict the appearance of the co-precipitates.

The composition of Alloy 706 deviates greatly from the area where the co-precipitates appear in the case of Alloy 718, as shown in Fig. 15^{25,27,30}. Therefore, it is suggested that the composition of the matrix also influence in the appearance of the co-precipitates. Namely, Fe/Ni ratio and presence of Mo exert influence on the stability of γ' and γ'' . Especially, it is known that "compact morphology" type co-precipitates are more excellent than the single phase γ' or γ'' in the elevated temperature property^{27,28,30,31}. So, it is possible to develop a new alloy with good high temperature characteristics by the compositional modification of Alloy 706.

It was considered that the appearance of co-precipitates passed following the process that, first, the γ' is generated and the γ'' by which γ' was made a core grows up while keeping the coherency²⁵⁻³². In this study, it was newly found out that the special coherency, which is $\gamma'-\gamma''-\gamma$, between either co-precipitates and the matrix was maintained as shown in Fig. 5 or Fig. 11. Therefore, it is strongly

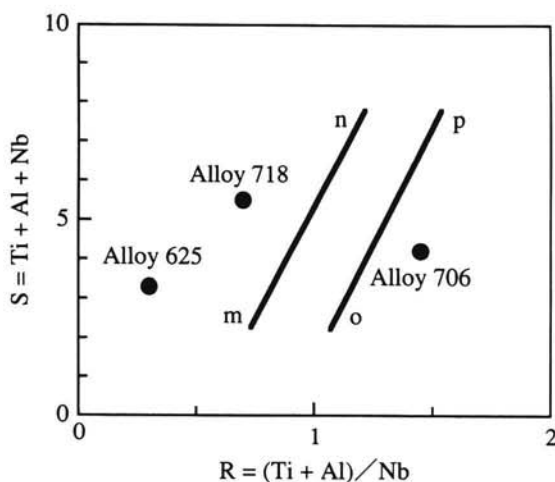


Fig. 15 S-R diagram of Alloy 718^{25,27,30}
In the diagram the area defined by m, n, o and p are the area where precipitation of $\gamma'-\gamma''$ co-precipitate is possible. Ti, Al, Nb are at.% of each element.

supported that the co-precipitates are actually formed through such a process.

On the other hand, it is necessary to shift the γ' precipitation area to short term side than γ'' precipitation area on the TTP diagram when the co-precipitates passes such a growth process. On the TTP diagram newly presented in this study, the precipitation of γ'' has begun before γ' appears in case of either "On Heating TTP" and "On Cooling TTP" diagrams. It is thought that the reason for the mismatch of γ and γ'' is to be larger than the mismatch of γ and γ'' . This fact also supports the formation of the co-precipitate with such a process. Accordingly, it can be concluded that the appearance of $\gamma'-\gamma''$ co-precipitates passed following the process that, first, the γ' is generated and the γ'' by which γ' was made a core grows up while keeping the coherency from the result of this study.

Moreover, it is estimated that whether the structure of co-precipitate becomes the double cuboidal structure or the overlaid structure depends on the size of γ' that had been generated before γ'' precipitate. The growth model of co-precipitate is shown in Fig. 16. According to the size of γ' which is initially precipitated, whether the precipitation becomes overlaid structure or double cuboidal structure is decided, that is the core of γ' completely covered with γ'' thin skin on its six plane or not covered²⁵.

It is thought that the difference of the size of γ'

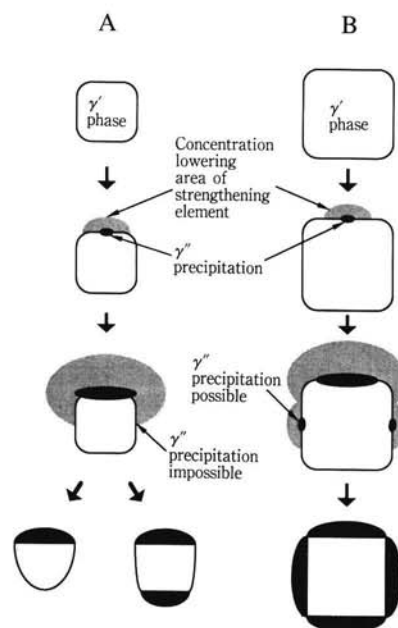


Fig. 16 Schematic diagram of growth mechanism in co-precipitates²⁵
A. Initially precipitated γ' is small
B. Initially precipitated γ' is large

in two kinds of co-precipitates is caused because the heat treatment stage where each co-precipitate appeared is different. The double cuboidal γ' - γ'' co-precipitates appeared after the stabilizing treatment of the three-step heat treatment. It is considered from "On Cooling TTP" diagram that γ' phase precipitated at stabilizing heat treatment or its temperature range just above and γ'' phase was formed around it at cooling after the stabilizing treatment. On the other hand, overlaid γ' - γ'' co-precipitates were formed at the aging treatment. In this case, it is considered from the "On Heating TTP" diagram that γ' phase appeared during the heating stage up to the aging treatment temperature, and γ'' phase precipitated on its periphery within the aging temperature. In other words, the areas of formation of γ' is estimated to be around 800°C in the case of double cuboidal type and around 600°C in the case of overlaid type.

In general, it is known that the growth rate of γ' in the Ni base superalloy follows the LSW theory of diffusion-controlled growth, and the growth of the spherical dispersed precipitated particle can be written as

$$\bar{r}^3 - \bar{r}_0^3 = K't \dots \dots \dots (1)$$

where \bar{r} is the average radius of the growing particle at time t , \bar{r}_0 is the radius at the onset of the coarsening process and K' is the rate constant^{33,34}. Also, it is shown that the (1) equation consists experimentally in many wrought superalloy and the activation energy of the growth rate constant is requested, too³⁵⁻³⁹. Although the detail of calculation is omitted here, estimating from the experimental result of γ' in Alloy 718³⁶ and γ' in A286³⁸, the growth rate of γ' at 800°C is about 5 to 10 times faster than that of 600°C. That is, the size of γ' that had been generated before γ'' precipitate is estimated to be about one order different. Therefore, it is thought that, when the precipitation of γ' takes place around 600°C, it becomes overlaid type and, when it occurs around 800°C, it becomes double cuboidal type.

4. Conclusions

As a Result of investigating precipitation behavior of Fe-Ni wrought superalloy 706 by a transmission electron microscopy in detail, the following conclusions are obtained.

(1) In the case of the two-step heat treatment, the precipitate in the grain matrix consists predominately of overlaid γ' - γ'' co-precipitates, and no precipitates are observed at the grain boundary.

(2) In the case of the three-step heat treatment, precipitation in the grain matrix reveals the appearance of double cuboidal γ' - γ'' co-precipitate in addition to the overlaid γ' - γ'' co-precipitate, and η phase precipitates at the serrated grain boundary accompanied by the denuded zone.

(3) Four type of precipitates appears η , γ' , γ'' and overlaid γ' - γ'' co-precipitate in the "On Heating TTP" diagram of Alloy 706.

(4) Five type of precipitates appears η , γ' , γ'' phase, overlaid γ' - γ'' co-precipitate and double cuboidal γ' - γ'' co-precipitate on the "On Cooling TTP" diagram of Alloy 706

References

- (1) E.E.Brown and D.R.Muzyka : Superalloys II, Ed. by C.T.Sims et al., John Wiley & Sons, New York, (1987), 165.
- (2) H.L.Eiselstein : ASM Tech. Rep., No.C70-9.5, (1970), 1.
- (3) H.L.Eiselstein : Met. Eng. Q., November (1971), 20.
- (4) E.L.Raymond and D.A.Wells : Proc. 2nd Int. Conf. on Superalloys-Processing, Metals and Ceramics Information Center, Columbus, (1972), N-1.
- (5) P.W.Shilke, J.J.Pepe and R.C.Schwant : Proc. Symp. on Superalloys 718, 625, 706 and Various Derivatives, Ed.by E.A.Loria, TMS, Warrendale, (1994), 1.
- (6) A.D.Helms, C.B.Adaszczik and L.A.Jackman : Proc. 8th Int. Symp. on Superalloys (Superalloys 1996), Ed.by R.D.Kissinger et al., TMS, Warrendale, (1996), 427.
- (7) J.H.Moll, G.N.Maniar and D.R.Muzyka : Met. Trans., 2(1971), 2143.
- (8) J.H.Moll, G.N.Maniar and D.R.Muzyka : *ibid.*, 2(1971), 2153.
- (9) L.Remy, J.Laniese and H.Aubert : Mat. Sci. Eng., 38(1979), 227
- (10) T.Takahashi, T.Ishiguro, K.Orita, J.Taira, T. Shibata and S.Nakata : Proc. Int. Symp. on Superalloys 718, 625, 706 and Various Derivatives, Ed.by E.A.Loria, TMS, Warrendale, (1994), 557.
- (11) W.L.Bell, T.Lauritzen, E.S.Darlin and R.W.Warner : ASTM STP., 611(1976), 353.
- (12) L.E.Thomas : US DOE Rep., No.HEDL-SA-2161, (1980).
- (13) E.R.Gilbert and B.A.Chin : ASTM STP., 870(1985), 52.
- (14) W.J.S.Yang and B.J.Makenas : ASTM STP., 870(1985), 127.

- (15) K.A.Heck : Proc. Int. Symp. on Superalloys 718, 625, 706 and Various Derivatives, Ed.by E.A.Loria, TMS, Warrendale,(1994), 393.
- (16) G.W.Kuhlman, A.K.Chakrabarti, R.A.Beaumont, E.D.Seaton and J.F.Radavich : *ibid.*, 441.
- (17) Inconel 706 : Undated brochure obtained from The International Nickel Company,(1974)
- (18) T.Shibata, Y.Shudo and Y.Yoshino: Jurnal of The Japan Institute of Metals, 60(1996),802.
- (19) T.Shibata, Y.Shudo, Y.Yoshiho. T.Takahashi and T.Ishiguro: *Tetsu-to-Haganê*, 82(1996),765.
- (20) T.Shibata, Y.Shudo, Y.Yoshino, T.Takahashi and T.Ishiguro: *Tetsu-to-Haganê*, 82(1996),853.
- (21) T.Shibata, Y.Shudo and Y.Yoshino : Proc. 8th Int. Symp. on Superalloys(Superalloys 1996), Ed. by R.D.Kissinger et al., TMS, Warrendale,(1996), 153.
- (22) T.Shibata, Y.Shudo, Y.Yoshino, T.Takahashi and T.Ishiguro : *ibid*, 627.
- (23) M.Kusuhashi and S.Nishiya: Pat.Pub.No.Hei6-240427
- (24) S.Li, J.Zhuang, J.Yang, Q.Deng, J.Du, X.Xie, B.Li, Z.Xu, Z.Cao, Z.Su and C.Jiang : Proc. Int. Symp. on Superalloys 718, 625, 706 and Various Derivatives, Ed.by E.A.Loria, TMS, Warrendale,(1994), 545.
- (25) R.Cozar and A.Pineau : *Met. Trans.*,4(1973), 47.
- (26) J.P.Collier, S.H.Wong, J.C.Phillips and J.K.Tien : Proc. 6th Int. Symp. on Superalloys(Superalloys 1988), Ed.by D.N.Duhl et al., The Metallurgical Society, Warrendale,(1988), 43.
- (27) E.Andrew, R.Cozar and A.Pineau : Proc. Int Symp. on Superalloy 718-Metallurgy and Applications, Ed.by E.A.Loria, TMS, Warrendale,(1989), 241.
- (28) E.Gou et al. : Proc. Int. Symp. on Superalloys 718, 625 and Various Derivatives, Ed.by E.A.Loria, TMS, Warrendale,(1991), 389.
- (29) E.Gou, F.Xu and E.A.Loria : *ibid.*, 397.
- (30) E.Andrieu, N.Wang, R.Mollis and A.Pineau : Proc. Int. Symp. on Superalloys 718, 625, 706 and Various Derivatives, Ed.by E.A.Loria, TMS, Warrendale,(1994), 695.
- (31) X.Xie, Q.Liang, J.Dong, W.Meng, Z.Xu, F.Wang, Y.Cai, J.Zhang, N.Wang, E.Andrieu and A. Pineau : *ibid.*, 711.
- (32) E.Gou, F.Xu and E.A.Loria : *ibid.*, 721
- (33) I.M.Lifshitz and V.V.Slyozov : *J.Phys. Chem. Solids*, 19(1961), 35.
- (34) C.Wagner : *Z.Electrochem.*, 65(1961), 581.
- (35) K.Kusabiraki, H.Nagahama, L.Wang and T. Ooka: *Tetsu-to-Haganê*, 75(1989),1354.
- (36) K.Kusabiraki, L.Wang, T.Ooka and K.Yamada: *Tetsu-to-Haganê*, 76(1990),1341.
- (37) K.Kusabiraki, S.Araie and T.Ooka: *Tetsu-to-Haganê*,78(1992),650.
- (38) K.Kusabiraki, Y.Takasawa and T.Ooka: *Tetsu-to-Haganê*,78(1992),1854.
- (39) K.Kusabiraki, X.Zhang and T.Ooka: *Tetsu-to-Haganê*, 79(1993), 113.